Available online at www.sciencedirect.com
ScienceDirect
Journal of Sound and Vibration 323 (2009) 173–193
JOURNAL OF SOUND AND VIBRATION
www.elsevier.com/locate/jsvi

Predicting changes in vibration behavior using first- and second-order iterative embedded sensitivity functions

Chulho Yang[a,*], Douglas E. Adams[b]

[a]*Mechanical Engineering Technology, Oklahoma State University, Stillwater, OK 74078, USA*
[b]*Mechanical Engineering, Purdue University, West Lafayette, IN 47907, USA*

Received 1 October 2007; received in revised form 3 December 2008; accepted 4 December 2008
Handling Editor: C.L. Morfey
Available online 14 January 2009

Abstract

In product manufacturing and test environments, engineers must predict how mechanical components will vibrate when design modifications are made to the mass, damping, or stiffness properties of the components. If component models are not available, then engineers must rely on test data from the initial component to conduct their design sensitivity analysis. Embedded sensitivity functions derived solely from test data have previously been applied to identify optimal design modifications for reducing linear vibration resonance problems in certain frequency ranges. However, forced response predictions were not accurate due to the nonlinear nature of the frequency response function variation for large design modifications. This paper develops two techniques for predicting the forced response of mechanical components for local changes in properties based on (a) first-order multi-step iterative prediction and (b) second-order iterative sensitivity functions. The methods are applied to a single degree of freedom analytical model to determine the accuracy of the predictions. Some tests and finite element analyses are conducted on a cantilever beam, a sub-system of an automotive vehicle, a structural component of a truck dumping system, and a lever arm with a modification to the mass distribution to demonstrate the feasibility of these predictions in experimental and analytical applications.

1. Introduction

1.1. Technical need

It is important in manufacturing to minimize the product development lifecycle. In the automotive industry, problems with NVH (noise, vibration, and harshness) are often found after prototypes are built and assembled into systems. Complete system models are not available to component suppliers for use in determining solutions to vibration and noise problems. Therefore, automotive suppliers use tests to diagnose problems by collecting forced dynamic response data at the system level. Then design iteration is used to identify a solution to those problems. This paper proposes an alternative means of conducting sensitivity analysis without the

*Corresponding author. Tel.: +1 405 744 3033; fax: +1 405 744 7399.
E-mail addresses: chulho.yang@okstate.edu (C. Yang), deadams@ecn.purdue.edu (D.E. Adams).

0022-460X/$ - see front matter © 2008 Elsevier Ltd. All rights reserved.
doi:10.1016/j.jsv.2008.12.016

Nomenclature

Symbols

C_j	j-th damping
C_{mn}	damping between DOFs j and k
f_i	input force
H_{jk}	frequency response function
K_j	j-th stiffness
K_{mn}	stiffness between DOFs m and n
M_j	j-th mass
$M_{m\underline{\Omega}}$	m-th mass
N	number of iterations
P_{mn}	parameter connecting m- and n-th DOF
y	displacement in physical coordinate
ω	angular frequency
DOF	degree(s) of freedom
FRF	frequency response function
MDOF	multiple degree of freedom
SDOF	single degree of freedom

need for design iteration. The method can be applied using only a few channels of system-level test data without a simulation model. Embedded sensitivity functions are estimated using frequency response function data acquired from the baseline component. These sensitivity relationships determine how the frequency response functions change as a function of mass, damping, and stiffness properties of a component. Predictions can be made regarding the modified dynamic forced response performance using these sensitivity functions.

To make accurate predictions, however, the sensitivity functions derived from test data must be properly applied to avoid errors. The underlying assumption made in deriving the first-order embedded sensitivity functions is that the changes in mechanical properties are small relative to the baseline properties. This paper predicts the modified frequency response functions using two different techniques. The first technique is based on an iterative approach whereby small step changes in mechanical design properties are made so that at each stage new sensitivity functions can be calculated to reduce bias errors in the prediction. The second technique is based on the derivation of second-order sensitivity functions, which are then applied to make unbiased predictions of the frequency response functions for the modified design in much less computational time and number of iterations.

1.2. Literature review

There have been many studies on the prediction of system response mainly by finite and boundary element methods, experimental modal analysis, sensitivity analysis, or analytical approaches for simple mechanical models.

Sensitivity analysis techniques have been developed and applied for system response prediction for various mechanical systems and structures. Most of these techniques have been developed using eigenvalue and eigenvector sensitivity functions. Pomazal and Snyder [1] developed a procedure for determining the eigenvalues and eigenvectors of a discrete linear-vibration system resulting from the addition or removal of a discrete element. The known characteristics of the original system were used to generate the modified characteristic equation directly without solving the modified eigenvalue problem explicitly. Hallquist [2] extended the modification theory for damped systems to determine the effects of mass modifications. Zimoch [3] presented a sensitivity analysis method for linear systems subject to variations in mechanical parameters. The system that was analyzed could be either conservative or non-conservative with or without an applied excitation. Lee et al. [4] proposed a numerical method that can find the eigenvalue and eigenvector derivatives of the structural and mechanical damped system by solving the algebraic equations with a symmetric coefficient matrix added as a side condition. Park et al. [5,6] used a substructure-coupling concept to derive the system equations that can be applied when large changes in the modal properties take place. The frequency response function matrices of the baseline and modified structures were coupled through the connection points under the force equilibrium and geometric compatibility condition to obtain more accurate modified modal properties. Ozguven [7,8] developed a frequency response function (FRF) based method to avoid matrix inversion or minimize the order of matrices involved in the computation for local modification.

An integrated finite element model of a passive structure, bonded active patch, and shunted circuit was utilized by Belloli et al. [9] for predicting structural resonant frequencies, optimum values for electric components, and the resulting vibration suppression performance. Sheng et al. [10] demonstrated a wavenumber-based modeling approach using finite/boundary element methods that can be used to predict ground vibrations from trains running either on the ground surface or in tunnels. Davis et al. [11] performed an experimental and numerical investigation into the static and dynamic responses of shape memory alloy hybrid composites (SMAHC) beams to study the feasibility of finite element modeling code to predict stiffness changes in the structure due to change in temperature. Chen et al. [12] also studied a prediction method for ground vibration induced by passing trains on bridge structures using two methods: a hybrid method involving a numerical model, field measurement, and assessment handbook; and a full numerical modeling method. Dalenbring [13] conducted finite element prediction of forced vibrations using a linear viscoelastic constitutive damping modeling technique.

The accuracy of prediction in most of this prior research is highly dependent on the accuracy of finite element modeling. These methods also require long calculation times and much experimental effort to obtain a high correlation between simulated and test data. These methods are especially challenging to apply for complex structures for which modeling uncertainties exist in structural parameters or boundary conditions.

There have also been many studies to resolve issues pertaining to limitations in the structural dynamic modification techniques including unmeasured rotational degrees of freedom and truncation of modes. Much research focus has been devoted to two main areas: developing techniques for the estimation of rotational degrees of freedom (DOF) and developing techniques to approximate realistic structural changes by using only the available measured translational DOF.

Avitabile et al. [14] studied the effect of rotational degrees of freedom for hybrid modeling applications. These researchers explained the effect of truncation of the rotational degree of freedom through a structural dynamic modification equation and by inspection of the frequency response function anti-resonances. Mottershead et al. [15,16] used an X-block attached to the system under investigation to estimate the full 6×6 receptance matrix. By estimating the full receptance matrix of the system including the rotational degrees of freedom, the modified system receptance of a structure in the form of a large overhanging mass could be predicted. Their work was based on earlier studies on the receptance method [17–20].

The goal of this study is to provide engineers with a technique that can be applied to realistic vibration problems using only the measured data to select structural dynamic modifications. NVH engineers usually have a limited time and design authority to change their product including limits on the space, weight, and cost. Because translational DOFs are most commonly measured, a technique that utilizes translational DOFs is examined in this paper.

The experimental embedded sensitivity functions [21–24] have been used to determine the variation in frequency response function magnitude and phase with respect to perturbations in mass, damping, and stiffness parameters. The embedded sensitivity functions are explicit functions of the frequency response functions; consequently, the individual mass, damping, and stiffness parameters are not needed to compute the sensitivity functions. These sensitivity functions in addition to the previous work mentioned above can only be used to describe changes in the frequency response for small perturbations in the system parameters. The approaches described below extend the embedded sensitivity functions to large perturbations in the component design.

2. Embedded sensitivity theory and application to a single degree of freedom system

2.1. Formulation of embedded sensitivity function for general case

Embedded sensitivity functions indicate the variation in frequency response function magnitude and phase with respect to perturbations in lumped mass, damping, and stiffness parameters. The sensitivity functions for $H_{jk}(\omega)$ with respect to the coupling parameter, P_{mn} (e.g., M_{m0}, C_{mn}, K_{mn}), are computed using the following equations after partial differentiation [14]:

$$\frac{\partial H_{jk}}{\partial K_{mn}} = -[H_{jm}(\omega) - H_{jn}(\omega)][H_{km}(\omega) - H_{kn}(\omega)] \text{ with } H_{j0}(\omega) \equiv 0, \tag{1a}$$

$$\frac{\partial H_{jk}}{\partial C_{mn}} = \mathrm{j}\omega \frac{\partial H_{jk}}{\partial K_{mn}}, \tag{1b}$$

$$\frac{\partial H_{jk}}{\partial M_{m0}} = (\mathrm{j}\omega)^2 \frac{\partial H_{jk}}{\partial K_{m0}}. \tag{1c}$$

Note that only measured response data, $H_{ij}(\omega)$, are needed to calculate embedded sensitivity functions. Also note that these formulae only apply for small changes in mass, damping, or stiffness. These functions have been applied to identify design modifications for eliminating noise and vibration problems in mechanical systems. These functions are used in this paper to predict the system response if a design modification is made causing a larger change in lumped mass, damping or stiffness parameters in the system.

2.2. Prediction for single degree of freedom system by first-order expansion

Taylor series expansions can be used to predict the new FRF of a dynamic system if a parameter (stiffness, damping or mass) in the system is modified. Eq. (2) shows a first-order Taylor series in terms of a small change, ΔK_{mn}, in stiffness parameter, K_{mn}:

$$H_{jk,1} \cong H_{jk,0} + \frac{\partial H_{jk}}{\partial K_{mn}} \Delta K_{mn}. \tag{2}$$

This equation is a linear relationship between the frequency response functions before ($H_{jk,0}$) and after the change ($H_{jk,1}$) in stiffness is made.

A single degree of freedom (SDOF) simulation example is analyzed using embedded sensitivity functions to demonstrate the use of Eq. (2) to predict the new FRF after making the stiffness modification. The SDOF system under investigation is shown in Fig. 1.

In Fig. 2, the FRF magnitude plots for the baseline SDOF system and new system with 2000 N/m higher stiffness are compared with a predicted magnitude plot that is generated using the embedded sensitivity function in Eq. (2). The Taylor series equation is accurate for small changes in parameters on the order of 1–2 percent; however, as the amount of change increases the accuracy of the prediction decreases as shown in Fig. 2. This decrease in accuracy is due to the fact that the amplitude and phase information of the sensitivity function is not updated after the stiffness parameter is modified. Therefore, the sensitivity function of the baseline system is different from that of the modified system. In this case, the response of the system with a 7000 N/m stiffness is predicted based on the sensitivity of the baseline system, which possesses a 5000 N/m stiffness (40 percent stiffness difference between baseline and modified systems).

2.3. Prediction by multi-stage sensitivity update (first-order Taylor series expansion)

To make the prediction of the system FRF more accurate, a new approach is proposed. This approach is to iterate on the system response in N steps. Instead of calculating the system response in one step, the magnitude of the parameter change is reduced by a factor of N to calculate the FRF and update the sensitivity function for every step in an iterative series of predictions. In Eq. (2), the embedded sensitivity function can be

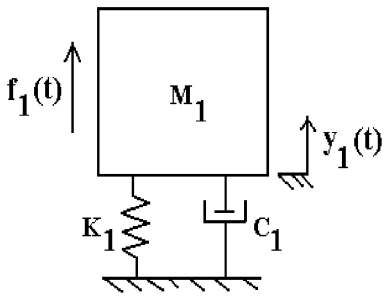

Fig. 1. Single degree of freedom model: $M_1 = 1$ kg, $K_1 = 5000$ N/m, $C_1 = 10$ N s/m.

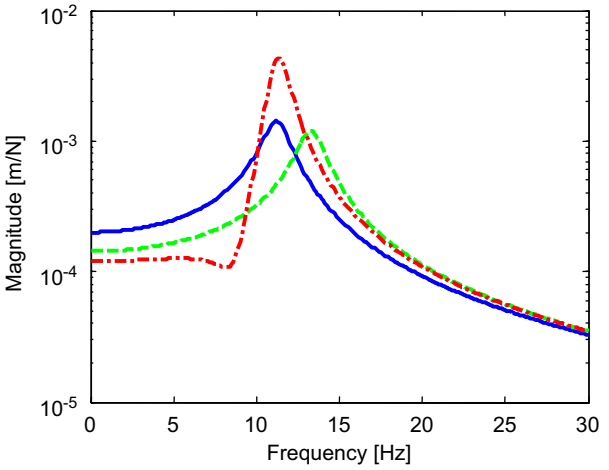

Fig. 2. Initial FRF with 5000 N/m (——), modified FRF with 7000 N/m (- - -), predicted FRF in 1 step (-.-.-).

expressed as shown in Eq. (3):

$$\frac{\partial H_{jk}}{\partial K_{mn}} = -(H_{mj} - H_{nj})(H_{mk} - K_{nk}). \tag{3}$$

Eq. (3) is the same as Eq. (1a) after exchanging subscripts corresponding to the input and output points for the FRFs. The exchange of these subscripts is acceptable assuming that reciprocity applies to the system of interest. The subscripts were exchanged in this manner to simplify the derivation of the following sensitivities and to reduce the number of test sets required for the sensitivity calculation. For example, if an excessive vibration issue involving a certain FRF, H_{jk}, needs to be resolved, only two sets of modal test data are needed with an input force at k and a response at j. However, the acceleration can be measured at as many points as are available (m and n). After the most promising design parameter is identified by the embedded sensitivity analysis, additional test sets with the excitation at those points can also be obtained for the prediction.

The new approach updates this embedded sensitivity function in N steps and this means that not only H_{jk} but also H_{mj}, H_{nj}, H_{mk}, and H_{nk} need to be updated at every step as well. To update those FRFs, more FRFs like H_{mm}, H_{mn}, H_{nm}, and H_{nn} need to be updated as a result. Although it requires a certain amount of data to calculate all of these updates, it is worthwhile to pursue this method because it is faster and still much less expensive than building many prototype parts for testing in order to identify the best design solution.

The ith FRF update can be expressed as shown in Eq. (4a)–(4d). Note that the increment in stiffness K_{mn} is divided by the iteration number N:

$$\begin{aligned} H_{mj,i} &\cong H_{mj,i-1} + \left(\frac{\partial H_{mj}}{\partial K_{mn}}\right)_{i-1} (\Delta K_{mn}/N) \\ &= H_{mj,i-1} + (H_{mm} - H_{nm})(H_{mj} - K_{nj})_{i-1}(\Delta K_{mn}/N), \end{aligned} \tag{4a}$$

$$\begin{aligned} H_{nj,i} &\cong H_{nj,i-1} + \left(\frac{\partial H_{nj}}{\partial K_{mn}}\right)_{i-1} (\Delta K_{mn}/N) \\ &= H_{nj,i-1} + (H_{mn} - H_{nn})(H_{mj} - K_{nj})_{i-1}(\Delta K_{mn}/N), \end{aligned} \tag{4b}$$

$$\begin{aligned} H_{mk,i} &\cong H_{mk,i-1} + \left(\frac{\partial H_{mk}}{\partial K_{mn}}\right)_{i-1} (\Delta K_{mn}/N) \\ &= H_{mk,i-1} + (H_{mm} - H_{nm})(H_{mk} - K_{nk})_{i-1}(\Delta K_{mn}/N), \end{aligned} \tag{4c}$$

$$H_{nk,i} \cong H_{nk,i-1} + \left(\frac{\partial H_{nk}}{\partial K_{mn}}\right)_{i-1} (\Delta K_{mn}/N)$$
$$= H_{nk,i-1} + (H_{mn} - H_{nn})(H_{mk} - K_{nk})_{i-1}(\Delta K_{mn}/N). \quad (4d)$$

From these updated FRFs, the embedded sensitivity of the system response to a modified parameter at each step is then expressed as shown in:

$$\begin{aligned}
\left(\frac{\partial H_{jk}}{\partial K_{mn}}\right)_i &= -(H_{mj} - H_{nj})(H_{mk} - K_{nk})_i \\
&= -\begin{bmatrix} H_{mj} - (H_{mm} - H_{nm})(H_{mj} - H_{nj})(\Delta K_{mn}/N) - H_{nj} \\ +(H_{mn} - H_{nn})(H_{mj} - H_{nj})(\Delta K_{mn}/N) \end{bmatrix} \\
&\quad \times \begin{bmatrix} H_{mk} - (H_{mm} - H_{nm})(H_{mk} - H_{nk})(\Delta K_{mn}/N) - H_{nk} \\ +(H_{mn} - H_{nn})(H_{mk} - H_{nk})(\Delta K_{mn}/N) \end{bmatrix} \\
&= -[H_{mj} - H_{nj} - (H_{mm} - H_{nm} - H_{mn} + H_{nn})(H_{mj} - H_{nj})(\Delta K_{mn}/N)] \\
&\quad \times [H_{mk} - H_{nk} - (H_{mm} - H_{nm} - H_{mn} + H_{nn})(H_{mk} - H_{nk})(\Delta K_{mn}/N)] \\
&= -(H_{mj} - H_{nj})[1 - (H_{mm} - H_{nm} - H_{mn} + H_{nn})(\Delta K_{mn}/N)] \\
&\quad \times (H_{mk} - H_{nk})[1 - (H_{mm} - H_{nm} - H_{mn} + H_{nn})(\Delta K_{mn}/N)] \\
&= -(H_{mj} - H_{nj})(H_{mk} - H_{nk})[1 - (H_{mm} - H_{nm} - H_{mn} + H_{nn})(\Delta K_{mn}/N)],^2 \quad (5)
\end{aligned}$$

where

$$\begin{aligned}
&[1 - (H_{mm} - H_{nm} - H_{mn} + H_{nn})(\Delta K_{mn}/N)]^2 \\
&\quad = 1 - 2(H_{mm} - H_{nm} - H_{mn} + H_{nn})(\Delta K_{mn}/N) \\
&\qquad + (H_{mm} - H_{nm} - H_{mn} + H_{nn})^2(\Delta K_{mn}/N)^2 \\
&\quad \cong 1 - 2(H_{mm} - H_{nm} - H_{mn} + H_{nn})(\Delta K_{mn}/N). \quad (6)
\end{aligned}$$

In Eq. (6), the last term of the second line is negligible because it can be assumed that the magnitude of this term is much smaller than the magnitudes of the other terms. This assumption is reasonable because at each step the difference in each FRF and the increment of stiffness are small. Therefore, Eq. (5) can be expressed as shown in Eq. (7) and it is comparable to the second-order sensitivity function derived in the next section:

$$\begin{aligned}
\left(\frac{\partial H_{jk}}{\partial K_{mn}}\right)_i &\cong -(H_{mj} - H_{nj})(H_{mk} - H_{nk}) \times [1 - 2(H_{mm} - H_{nm} - H_{mn} + H_{nn})(\Delta K_{mn}/N)] \\
&\cong -(H_{mj} - H_{nj})(H_{mk} - H_{nk}) \\
&\quad + 2(H_{mj} - H_{nj})(H_{mk} - H_{nk})(H_{mm} - H_{nm} - H_{mn} + H_{nn})(\Delta K_{mn}/N). \quad (7)
\end{aligned}$$

The first term of Eq. (7) is the same as the first-order embedded sensitivity and the second term is the first-order embedded sensitivity multiplied by a combination of additional FRFs related by the design parameter to be changed and the increment in stiffness of the parameter at each step in the iteration. Consequently, a first-order Taylor series expansion of the predicted FRF can be expressed as follows:

$$\begin{aligned}
H_{jk,i+1} &\cong H_{jk,i} + \left(\frac{\partial H_{jk}}{\partial K_{mn}}\right)_i (\Delta K_{mn}/N) \\
&\cong H_{jk,i} - (H_{mj} - H_{nj})(H_{mk} - K_{nk}) \\
&\quad \times [1 - 2(H_{mm} - H_{nm} - H_{mn} + H_{nn})(\Delta K_{mn}/N)]_{i-1}(\Delta K_{mn}/N). \quad (8)
\end{aligned}$$

Eq. (8) shows that the predicted FRF in N steps is the accumulation of FRFs calculated at each step.

This approach was applied to a SDOF model again to investigate the performance in terms of prediction accuracy. As shown in Fig. 3, the predicted FRF in 100 iterations is nearly equal to the new FRF obtained

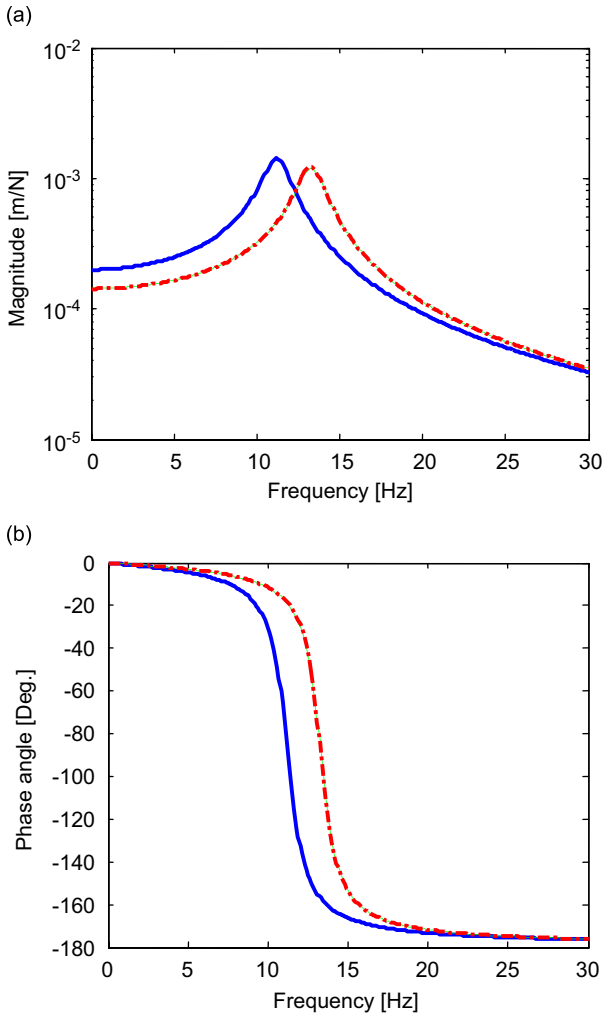

Fig. 3. (a) Magnitude and (b) phase angle of the initial FRF with 5000 N/m stiffness (——), modified FRF with 7,000 N/m stiffness (- - -) , predicted FRF in 100 steps iteration from the initial FRF (-.-.-).

when the higher stiffness is used in the system model. Recall that the predicted result contained large errors in the previous section so it can be concluded that the result obtained using this iterative approach is much improved.

2.4. Prediction by the second-order Taylor series expansion and embedded sensitivity function

By updating sensitivity information with iterative calculations, a more accurate prediction can be made. However, this approach requires many calculations. To obtain improved accuracy prediction using a smaller number of calculations, the second-order Taylor series expansion is used as expressed in Eq. (9). This expression indicates that the change in sensitivity information is also considered and updated by the second-order sensitivity calculation.

$$H_{jk,1} \cong H_{jk,0} + \frac{\partial H_{jk}}{\partial K_{mn}} \Delta K_{mn} + \frac{1}{2!} \frac{\partial^2 H_{jk}}{\partial K_{mn}^2} \Delta K_{mn}^2. \tag{9}$$

The second-order embedded sensitivity function can be derived as shown:

$$\frac{\partial^2 H_{jk}}{\partial K_{mn}^2} = \frac{\partial}{\partial K_{mn}}\left(\frac{\partial H_{jk}}{\partial K_{mn}}\right) = -\frac{\partial}{\partial K_{mn}}[H_{mj}(\omega) - H_{nj}(\omega)][H_{mk}(\omega) - H_{nk}(\omega)]$$
$$= 2[H_{mm}(\omega) - H_{mn}(\omega) - H_{nm}(\omega) + H_{nn}(\omega)][H_{mj}(\omega) - H_{nj}(\omega)][H_{mk}(\omega) - H_{nk}(\omega)]. \quad (10)$$

Note that this equation is in the same form as the first-order iterative embedded sensitivity functions shown in the previous section. It is reasonable that the second-order sensitivity function, which is the sensitivity to the first-order sensitivity functions, is close to the sensitivity update at every fine step. It can be concluded that iteration of the sensitivity calculation in N steps is equivalent to considering the trend of the sensitivity change using the derivative of the sensitivity function, i.e. the second-order sensitivity function.

Therefore, a second-order Taylor series expansion of a FRF can be written as follows:

$$H_{jk,1} \cong H_{jk,0} + \frac{\partial H_{jk}}{\partial K_{mn}}\Delta K_{mn} + \frac{1}{2!}\frac{\partial^2 H_{jk}}{\partial K_{mn}^2}\Delta K_{mn}^2$$
$$= H_{jk,0} - (H_{mj} - H_{nj})(H_{mk} - H_{nk})\Delta K_{mn}$$
$$+ (H_{mm} - H_{mn} - H_{nm} + H_{nn})(H_{mj} - H_{nj})(H_{mk} - H_{nk})\Delta K_{mn}^2$$
$$= H_{jk,0} - (H_{mj} - H_{nj})(H_{mk} - H_{nk})[1 - (H_{mm} - H_{mn} - H_{nm} + H_{nn})\Delta K_{mn}]\Delta K_{mn}. \quad (11)$$

The second-order sensitivity term is also purely a function of FRFs. Similar to the first-order iterative approach, more FRFs must be updated. However, the accuracy of the second-order calculation is much higher than for the first-order sensitivity as shown in Fig. 4. This improved accuracy is due to the fact that the second-order sensitivity calculation explicitly contains the change in the sensitivity information. Fig. 4 shows the initial and modified FRFs curves of the system and two predicted FRFs by first and second-order sensitivity functions calculated in 10 steps. For the first-order sensitivity prediction, the distortion in amplitude and phase information occurs around the resonance peak and these errors are due to the incorrect sensitivity information associated with the system possessing different values of the parameters (stiffness or mass).

Similarly, the number of calculations for the second-order sensitivity method is much less than for the first-order method to obtain the same level of accuracy as shown in Fig. 5. This plot compares the predicted FRFs using the first-order sensitivity in 100 iterations and the second-order sensitivity in 10 iterations with the calculated FRF curve for the modified system. As shown in this graph, the prediction by the second-order sensitivity method requires fewer numbers of iterations (1/10 in this case).

For this SDOF model, a direct calculation in one step was accurate enough for the small amount of change in stiffness below 1 percent. However, as the stiffness change becomes higher, more iterations are necessary to produce an accurate prediction. The comparison of iteration numbers for first- and second-order embedded sensitivity calculation for the same amount of accuracy, 0.1 Hz frequency and 1 percent in amplitude in this case, is shown in Fig. 6. Note that the first-order calculation requires much more iteration than the second-order one as the change in stiffness increases: for example, the number of iterations in the first-order sensitivity function for the system with 10 percent increase in stiffness is 10 times larger than for the second-order function. This result proves the effectiveness and accuracy of the second-order embedded sensitivity functions for system response prediction.

In a similar way, the FRF changes in terms of the mass change are shown in Fig. 7. The number of iterations for the second-order sensitivity function required to produce the same level of accuracy as obtained with the first-order function is about one third in this case.

3. Application of iterative embedded sensitivity to predict system response

3.1. Cantilever beam

To verify the applicability of the technique to realistic structures, a test was conducted for a cantilever beam as shown in Fig. 8. This beam is $540 \times 50 \times 1.2$ mm and made of stainless steel 409. One side of the beam is clamped and the other side is free. An impact hammer (PCB 086B03, sensitivity 2.14 mV/N) was used to excite

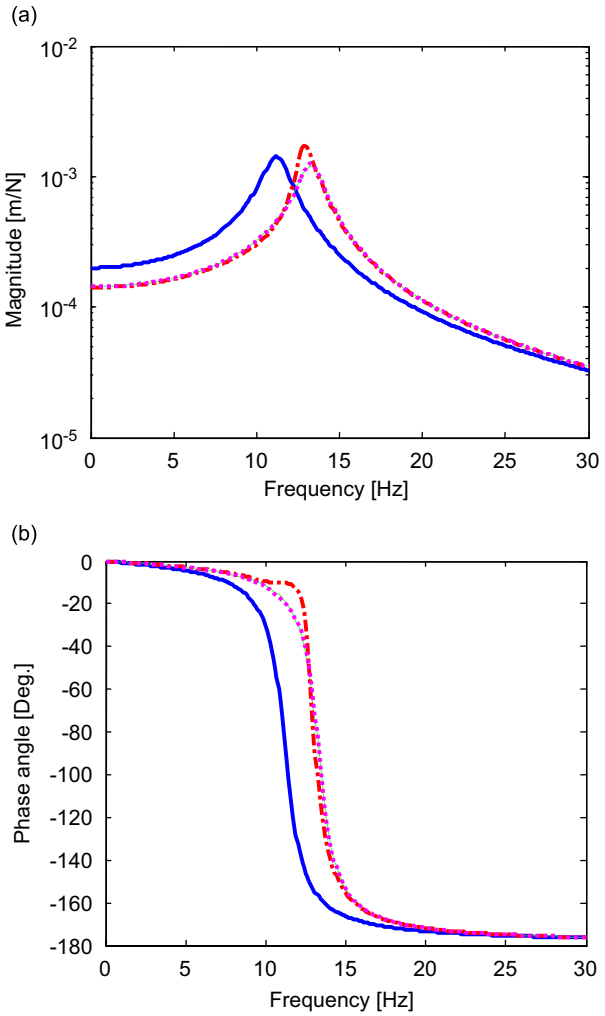

Fig. 4. (a) Magnitude and (b) phase angle of the initial FRF with 5000 N/m stiffness (——), modified FRF with 7000 N/m stiffness (- - -), predicted FRF in 10 steps (first-order sensitivity, -.-.-), predicted FRF in 10 steps (second-order sensitivity, ….).

the beam into vibration and six accelerometers (PCB model 356B21, sensitivity 9–10 mV/g, B&K 4508 001, sensitivity 9–10 mV/g) were used to measure the acceleration at each point. FRFs were measured and computed using LMS CADA-X software and the sensitivity calculation was performed using MATLAB V7. To obtain a full set of test data, impact forces were applied to six sensor locations one after the other.

The sensitivities of the beam to the first four mass parameters are shown in Fig. 9. Note that the parameter that causes the largest change in the FRF for each peak is different for each peak. Therefore, depending on the problem frequency, the most appropriate parameter should be selected and modified.

To simulate a design modification process to address a prototypical vibration problem, a 0.07 kg lumped mass was added to point 3 as shown in Figs. 10 and 11 compare the FRFs before and after the modification was applied with predicted FRFs using the first- and second-order embedded sensitivity functions. 10 iterations were calculated for the second-order embedded sensitivity functions and 30 iterations for the first-order function. When only 10 iterations were used for the first-order sensitivity, the predicted FRF curve was distorted as already shown in the SDOF model.

Note that the first four peaks are predicted very accurately and there are distortions on the fifth and sixth peaks. These distortions seem to be caused by some anomalous data near 240 and 360 Hz in the phase angle plot shown in Fig. 12. The system may have some minor resonance peaks at these frequencies, which are not

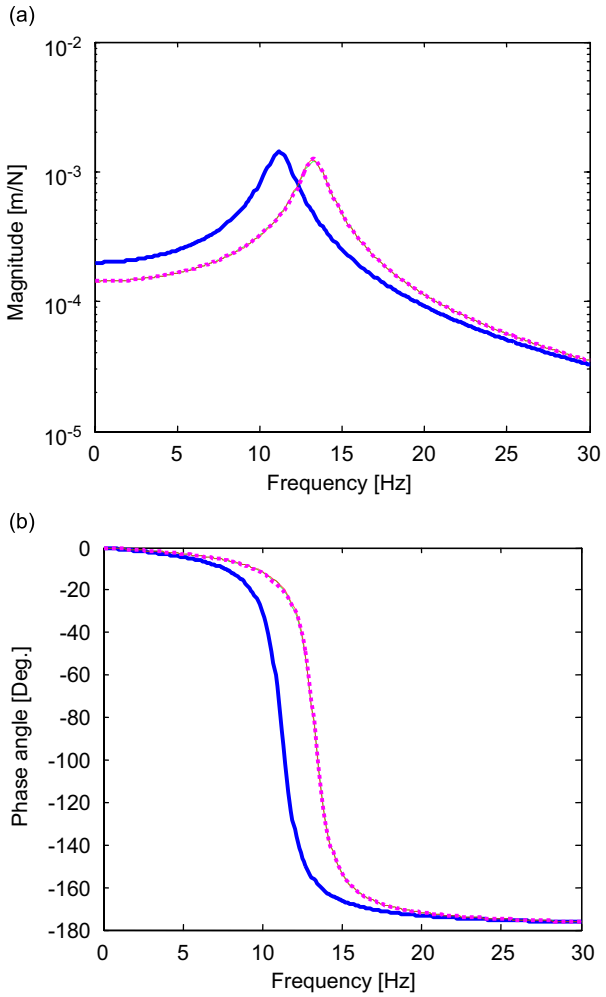

Fig. 5. (a) Magnitude and (b) phase angle of the initial FRF (——), modified FRF (- - -), predicted in 100 steps (first-order, -.-.-), predicted in 10 steps (second-order, ….).

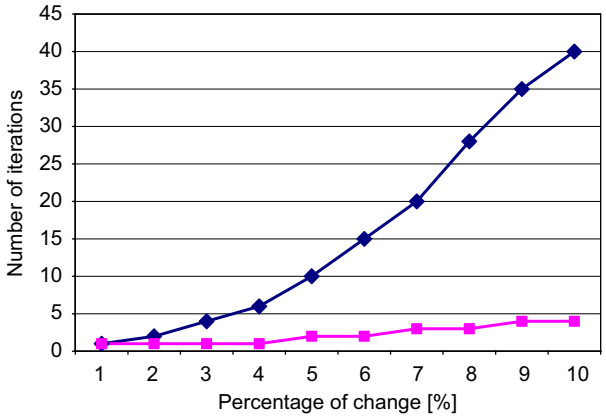

Fig. 6. Comparison of iteration numbers in first- (diamond) and second (square)- order embedded sensitivity calculation for the same level of accurate calculation: frequency within 0.1 Hz, amplitude within 1 percent.

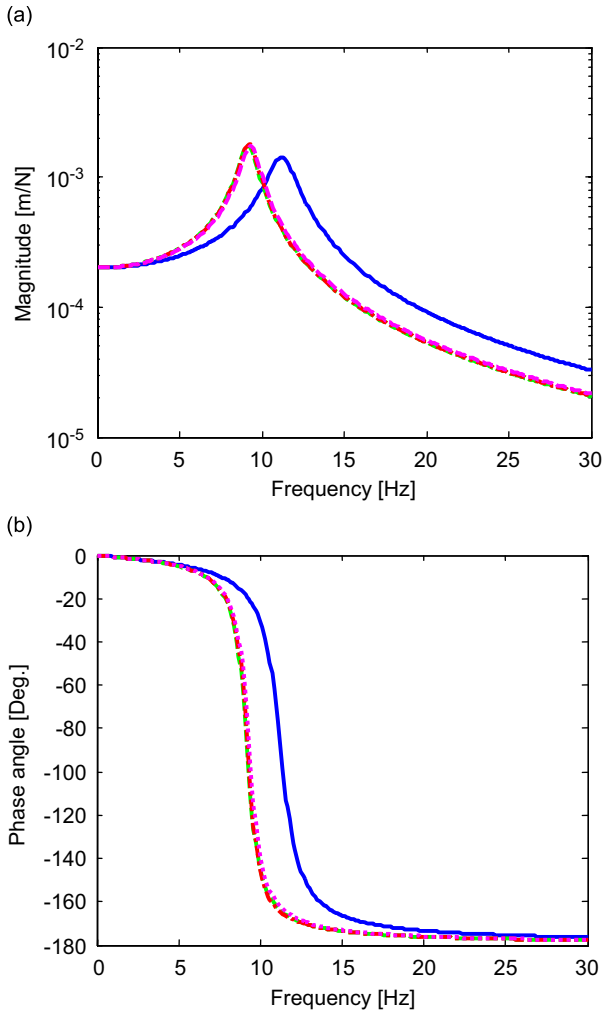

Fig. 7. (a) Magnitude and (b) phase angle of the initial FRF with 1 kg mass (——), modified FRF with 1.5 kg mass (- - -), predicted FRF in 60 steps (first-order, -.-.-), predicted FRF in 20 steps (second-order, …).

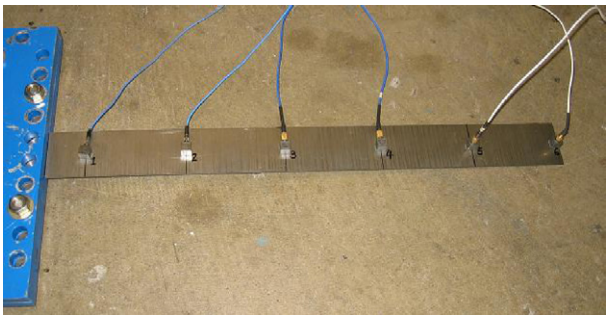

Fig. 8. A cantilever beam with accelerometers at six points.

dominant in this range or they may be caused by some measurement or processing error due for example to the accelerometer cable dynamics.

Note that the sensitivity calculation is based completely on the baseline system test results. Therefore, the predicted FRF curves tend to retain all characteristics (like number and order of peaks and dips) from the

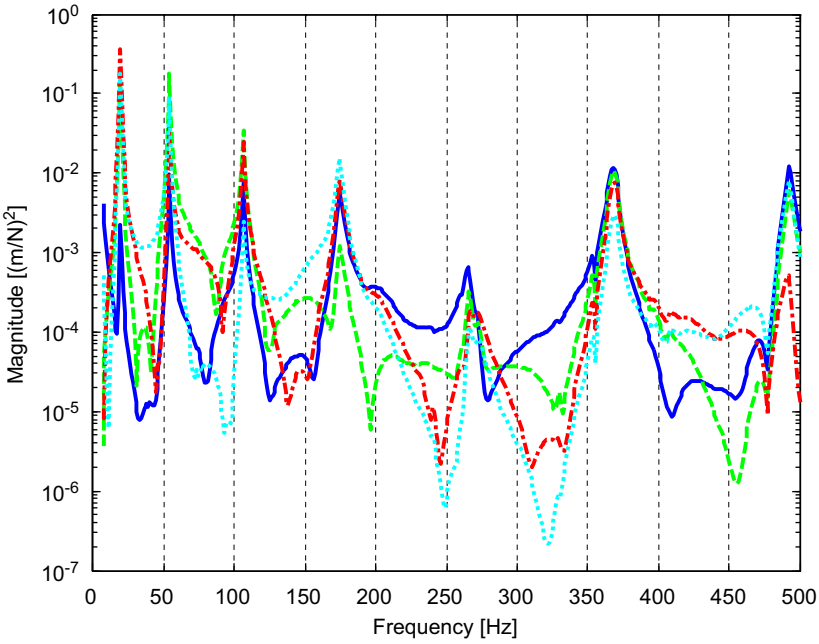

Fig. 9. Embedded sensitivity functions of the cantilever beam to the first four mass parameters.

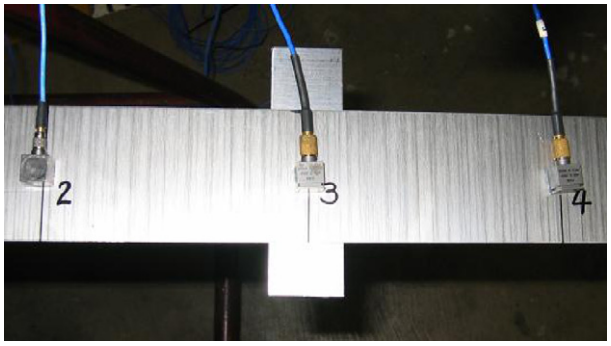

Fig. 10. Cantilever beam with 0.07 kg lumped mass added to point 3.

baseline system regardless of whether those characteristics are due to the system or a measurement error. More study on properties caused by measurement errors will be done in the near future. At this stage, it can be concluded that careful measurement and data processing should be done to reduce possible errors in prediction. Various modal analysis techniques will be investigated in the future to produce high quality predictions for the modified system FRFs. This approach is appropriate because multiple parameters in the system must be considered when the FRF is predicted. For example, in a case where a reinforcement bracket is welded to a system to stiffen a certain area, the change in mass caused by this bracket must also be considered in the prediction.

3.2. *A frame for a truck dumping system and a lever arm*

A welded structure of steel frames was analyzed using the finite element method shown in Fig. 13. This structure is composed of $50 \times 50 \times 1000$ mm frames, $50 \times 5 \times 200$ mm cross members, and a $200 \times 200 \times 10$ mm plate. Frequency response functions were obtained from ANSYS ver. 11 and sensitivity functions were computed using MATLAB V7. To obtain a full set of test data, input forces of 100 N were

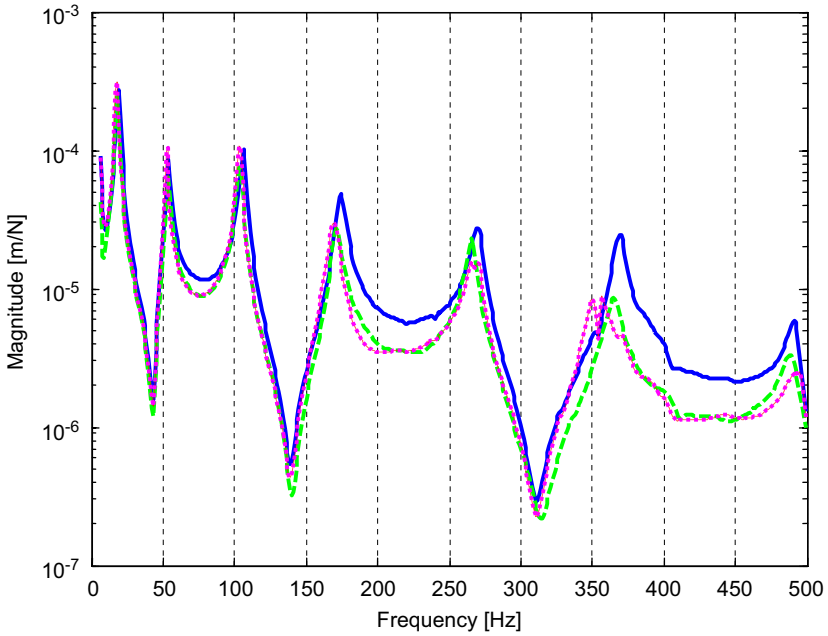

Fig. 11. Comparison of FRFs (H_{31}) before and after the modification in mass at point 3 with two predicted curves (first- and second-order embedded sensitivity functions).

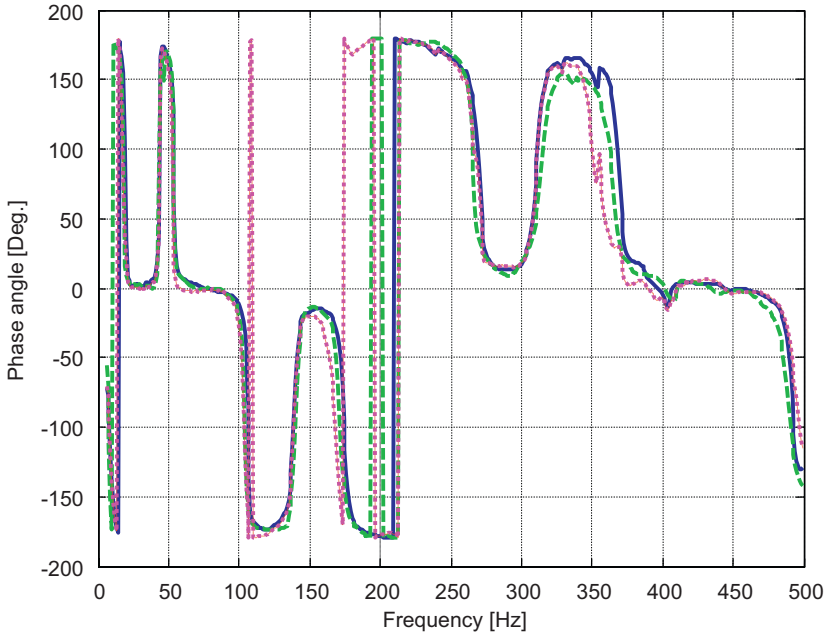

Fig. 12. Phase angle plots of initial, modified, and two predicted FRFs by the first- and second-order embedded sensitivity functions.

applied to four cross members with a fixed boundary condition at the plate. Due to the geometry of the structure, the dynamic response in the transversal direction (vertical direction in the figure) was examined in the frequency range from 0 to 300 Hz. After the most effective parameter was selected using sensitivity analysis, a steel block of $80 \times 50 \times 30$ mm (0.942 kg) mass was attached to the last cross member (the tip of the frame) as shown in Fig. 14. FRF H_{41} of the modified structure was obtained by FEA once again and then

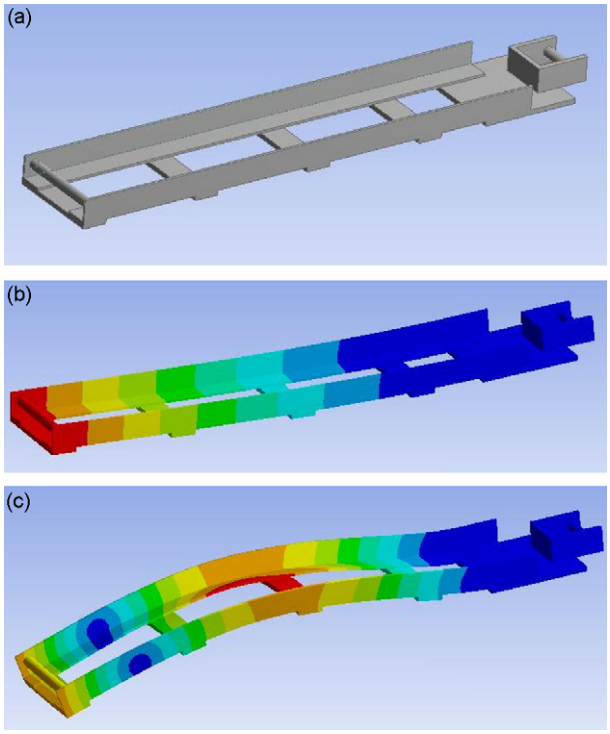

Fig. 13. A frame investigated by finite element analysis (a) and the mode shapes showing bending mode at 37 Hz (b) and 227 Hz (c).

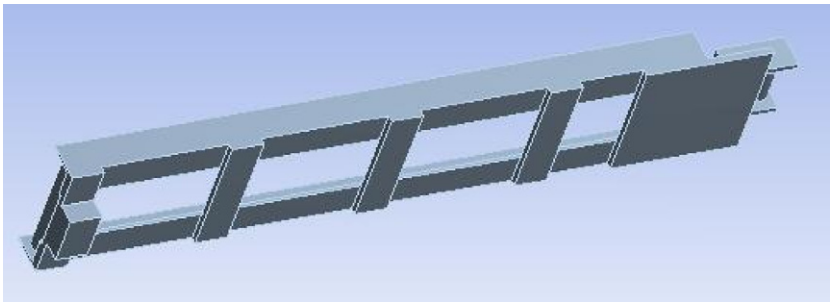

Fig. 14. A frame with mass 0.942 kg in the middle of the end member (left in the picture) of the structure.

compared with the predicted response using sensitivity functions in Fig. 15. Note that the exact change of 0.942 kg in mass was used to calculate the predicted FRF and this curve is exactly on top of the FRF obtained using FEA.

To investigate the limit of this technique, the same size block was added to the side frame instead of the center point of a cross member as shown in Fig. 16 to introduce additional DOF. Fig. 17 shows the comparison of FRFs again. This time, two additional peaks can be found on the modified FRF curve that were not observed in the baseline FRF. Those peaks were introduced by offsetting the block from the centerline of the structure. Note that the predicted curve does not contain these additional peaks because it is calculated based on the baseline (translational) system response. However, the pre-existing peaks were still accurately predicted. This kind of design modification would not be a practical solution because it introduces additional vibration issues due to asymmetry and occupies additional space. The example does demonstrate the limits of this technique.

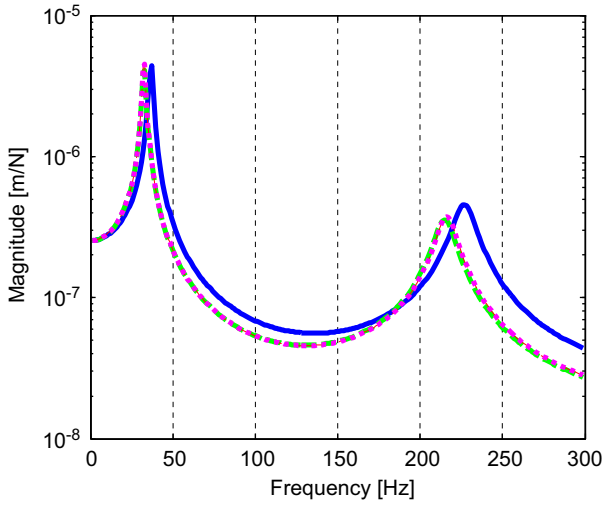

Fig. 15. FRF prediction for change in mass (0.942 kg) at the tip of the structure (in the middle of a cross member) by using sensitivity functions: frequency response of the initial structure (—), the modified structure (- - -), and the predicted one by sensitivity analysis (…).

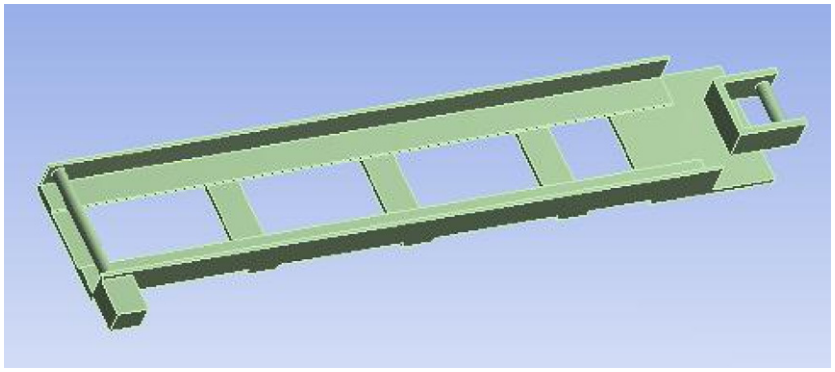

Fig. 16. A frame with mass 0.942 kg on the side of the end member (left in the picture) of the structure.

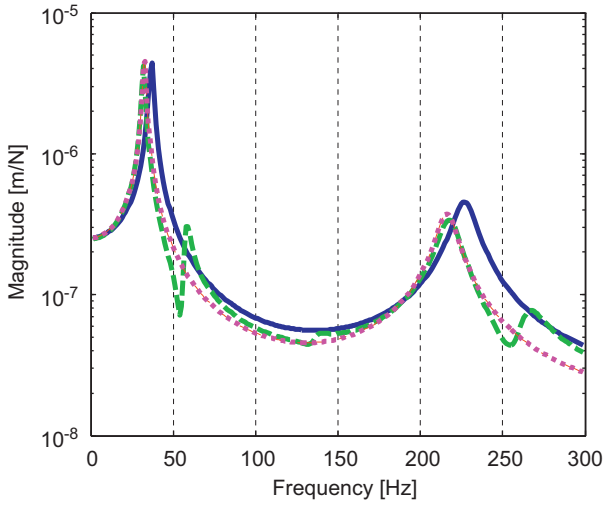

Fig. 17. FRF prediction for change in mass (0.942 kg) at the tip of the structure (on the side frame) by using sensitivity functions: frequency response of the initial structure (—), the modified structure (- - -), and the predicted one by sensitivity analysis (…).

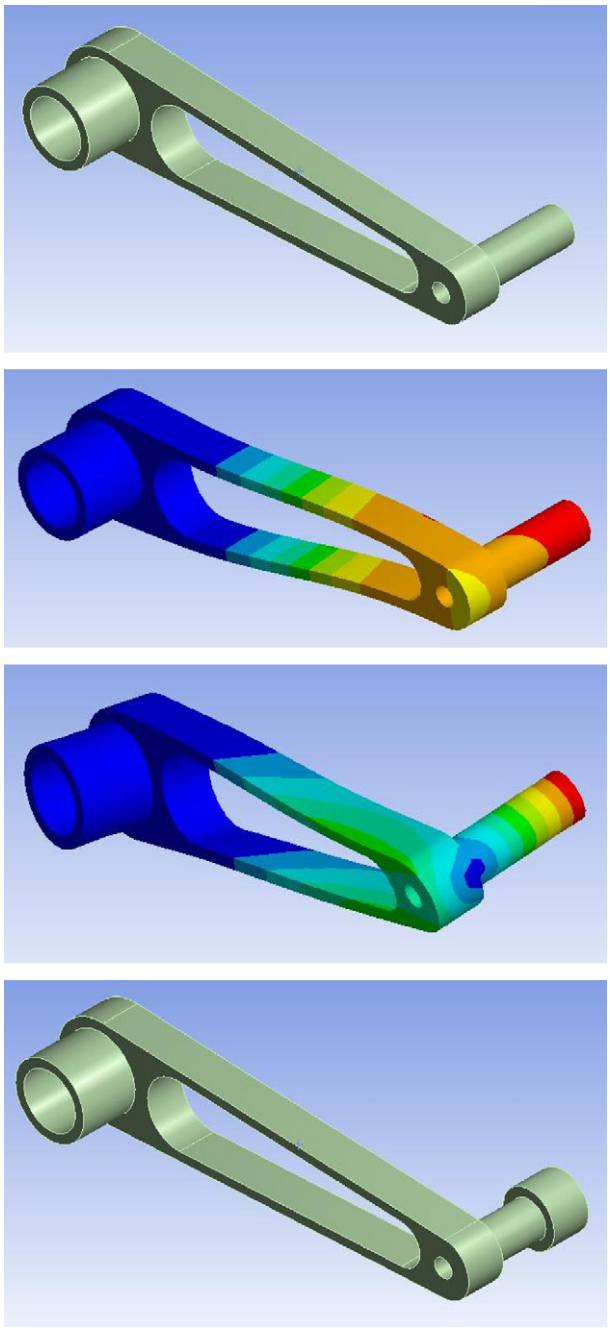

Fig. 18. A lever arm investigated by finite element method (a), the mode shapes at 212 Hz (b) and 610 Hz (c), and the modified structure with the mass at the right end.

Another structural component was studied to simulate the case with a twisting (or rotational DOF) mode in the original system shown in Fig. 18(a–c). A twisting mode shape at the tip of the structure due to the geometry is observed. However, only translational DOF are considered when performing the sensitivity calculation. If the mass of each measurement point can be regarded as a point mass, then translational measurements provide a reasonably accurate description of the dynamic response. Translational measurements are not sufficient for the case of a large component with a high moment of inertia. As in the previous example, the most effective parameter was selected and modified as shown in Fig. 18(d). Note that there is a

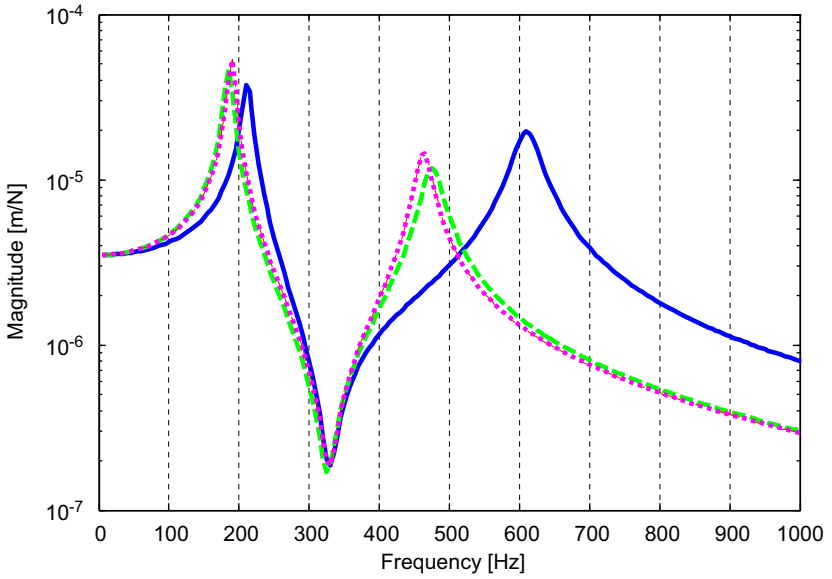

Fig. 19. FRF prediction for change in mass (0.07 kg) at the tip of the structure by using sensitivity functions: frequency response of the initial structure (—), the modified structure (- - -), and the predicted one by sensitivity analysis (…).

small discrepancy in the predicted and calculated response using FEA as shown in Fig. 19. The predicted result indicates more change from the initial structure than the calculated result. This discrepancy may be caused by the mass distribution of the added mass because the prediction process assumes that this mass is concentrated at the measurement point leading to higher effective mass at that point. This discrepancy increases as the volume of the mass increases.

It can be concluded that the accuracy of the prediction is high as long as the system response can be reasonably described using translational measurement DOF only and the design modification does not change the dynamic properties of the system. If the design modification increases or decreases the DOF (adds or removes rotational DOF), then the accuracy will be reduced.

3.3. An automotive sub-system

A sub-system of an automotive vehicle was tested as shown in Fig. 20. Note that this component has many areas that flex causing torsional modes. The goal of this test is to mitigate excessive vibration due to the resonance between a sub-system and engine firing frequencies to avoid interior noise at idle. In general, all sub-systems should be designed to avoid resonance frequencies that are aligned with excitations from the power train. For vehicles with four cylinder engines, the second- and fourth- order engine harmonics are the main contributors to vibration and noise from the power train. For example, if the engine idle is set to 650 rev/min, the natural frequencies of sub-systems should not be near 21.5 and 43 Hz. The system originally had natural frequencies close to those second- and fourth- order engine components. Modal testing on this system was conducted and embedded sensitivity functions were used to find the most appropriate design modifications and to predict the system response. The test result using the modified design was compared with the predicted result.

A 50 lbf electrodynamic shaker was instrumented with a PCB 288D01 impedance head (sensitivity 102.2 mV/lbf, 98.4 mV/g) for measuring force and acceleration at the attachment location and was used to excite the system into vibration to simulate the input from the power train. Accelerometers (PCB model 356B21, sensitivity 9–10 mV/g, B&K 4508 001, sensitivity 9–10 mV/g) were used to measure the acceleration at each point. FRFs were measured and computed using LMS CADA-X software and the sensitivity calculation was performed using MATLAB V7. To obtain a full set of test data, input forces were applied to four sensor locations 1, 7, 14, and 18. After the measurement of the baseline system, the FRFs were analyzed and

Fig. 20. An exhaust system tested for reduction of vibration at engine idle and lumped mass attached to the system.

sensitivity functions were calculated as shown in Fig. 21. Design parameter 1 was the most effective for modifying the vibration response. A lumped mass of 1.5 kg (3.39 lb shown in Fig. 20) was added to this point and FRFs were measured again for comparison with the predicted result as shown in Fig. 22. The shifts in natural frequencies 21 and 40 Hz were predicted with relatively high accuracy. Measured frequencies of the modified system were at 19 and 36 Hz, whereas the predicted ones were at 19.5 and 34 Hz.

Based on the test data examined in the cantilever beam and exhaust system, it can be concluded that the frequency shifts at the resonance peaks are accurately predicted but the responses at the anti-resonance remain the same as in the baseline system. This result demonstrates that the suggested technique can be accurately applied to structures with well-separated modes. However, this result also limits the application of this technique to design changes that do not shift the resonant frequency past the anti-resonant frequency. This phenomenon is caused by the low sensitivity of the system response to the design parameter suggesting that the effect of any change in stiffness or mass will vanish through the multiplication of an infinitesimal value of the sensitivity. Another issue is observed in the peak above 65 Hz. For this peak, the embedded sensitivity did not predict the response of the modified system. This error may be caused by the low amplitude of the peak. This peak has a low sensitivity and a high noise to signal ratio, which will be examined in future work.

4. Conclusions and future work

The second-order embedded sensitivity function described in this paper is a newly derived iterative approach for the prediction of forced vibration behavior in mechanical systems. The method is demonstrated in a numerical study on a SDOF linear model, in tests on a cantilever beam and an automotive exhaust system, and finite element analyses on a steel frame and a lever arm. In this study, only mass parameters were considered to simplify the measurements required and to ensure an accurate comparison with easily measured

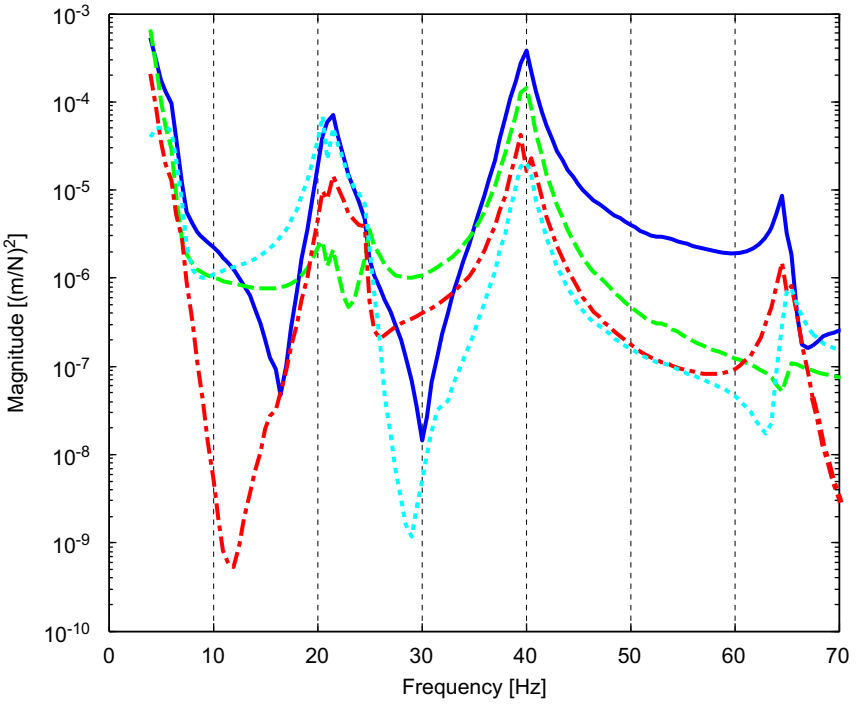

Fig. 21. Sensitivity of H_{11} to each mass parameters: sensitivity to parameter 1 (—), parameter 7 (- - -), parameter 14 (-.-.-), and parameter 18 (…). The sensitivity to parameter 1 is the highest for both at 21 and 40 Hz.

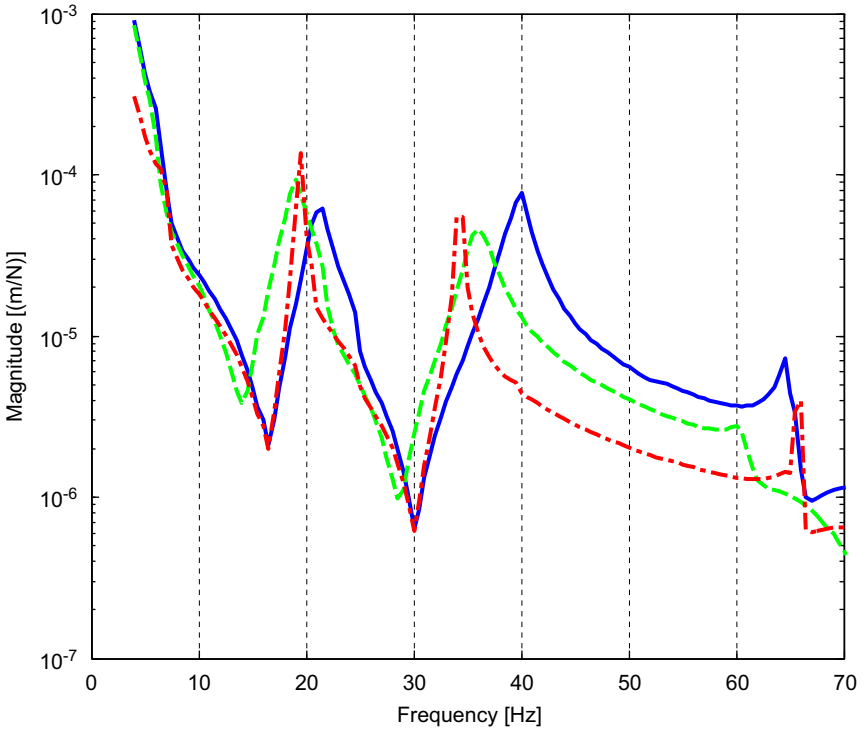

Fig. 22. Comparison of frequency response functions (FRFs): H_{11} of the initial system (—), modified system (- - -), and predicted system (-.-.-).

mass data; however, stiffness parameters exhibit the same results. The first- and second-order embedded sensitivity functions are computed for each parameter increment to accurately predict the modified FRF iteratively. The second-order embedded sensitivity functions are shown to predict the modified FRF more accurately using less iteration. This technique can save time in vibrations engineering by identifying the amount of a parameter change that is necessary to produce a desired change in the forced response of a mechanical system without building and testing excessive numbers of prototypes. The main advantage of this technique is that the identification of the best design parameter and the prediction of the system response can be achieved quickly in one step by using the same test data sets. Another advantage is that this technique is based on FRFs and does not need fully populated parameter matrices associated with the system being studied. However, this technique also has limitations to be addressed in the future. The magnitude of the design parameter change is limited to cases where no rotational DOF is involved and where the shifted resonance frequency does not pass the adjacent anti-resonances.

In the case of a system with pure response data without any noise in the measurement, as in numerical simulations and finite element analyses, the predicted results were accurate.

At this stage only one parameter was considered to predict the system response. However, it is necessary to extend the suggested approach to all major parameters for more accurate prediction of the system response. The approach that is being pursued to conduct this type of analysis is to use multi-variable Taylor series that take into account parameter changes that affect the entire frequency range of interest. A study to expand this technique to systems with rotational DOFs needs to be done for various and more practical applications.

Acknowledgements

The authors gratefully acknowledge Anthony Hicks, Director of System Engineering with EMCON Technology and Hao Jin, Chief Engineer for supporting this research. The experiments described in the paper were carried out at the EMCON Technologies Technical Center in Columbus, IN.

References

[1] R. Pomazal, V. Snyder, Local modifications of damped linear systems, *AIAA Journal* 9 (1971) 2216–2221.
[2] J. Hallquist, An efficient method for determining the effects of mass modifications in damped systems, *Journal of Sound and Vibration* 44 (1976) 449–459.
[3] Z. Zimoch, Sensitivity analysis of vibrating systems, *Journal of Sound and Vibration* 115 (1987) 447–458.
[4] I. Lee, D. Kim, G. Jung, Natural frequency and mode shape sensitivities of damped systems—part 1, distinct natural frequencies, *Journal of Sound and Vibration* 223 (1999) 399–412.
[5] Y.H. Park, Y.S. Park, Structure optimization to enhance its natural frequencies based on measured frequency response functions, *Journal of Sound and Vibration* 229 (2000) 1235–1255.
[6] Y.H. Park, Y.S. Park, Structural modification based on measured frequency response functions: an exact eigenproperties reallocation, *Journal of Sound and Vibration* 237 (2000) 411–426.
[7] H.N. Ozguven, A new method for harmonic response of non-proportionally damped structures using undamped modal data, *Journal of Sound and Vibration* 117 (1987) 313–328.
[8] H.N. Ozguven, Structural modifications using frequency response functions, *Mechanical Systems and Signal Processing* 4–1 (1990) 53–63.
[9] A. Belloli, D. Niederberger, S. Pietrzko, M. Morari, P. Ermanni, Structural vibration control via R-L shunted active fiber composites, *Journal of Intelligent Material Systems and Structures* 18 (2007) 275–287.
[10] X. Sheng, C.J.C. Jones, D.J. Thompson, Prediction of ground vibration from trains using the wavenumber finite and boundary element methods, *Journal of Sound and Vibration* 293 (2006) 575–586.
[11] B. Davis, T. Turner, S. Seelecke, Measurement and prediction of the thermomechanical response of shape memory alloy hybrid composite beams, *Journal of Intelligent Material Systems and Structures*, Published OnlineFirst, JIM 073172, 2007.
[12] Y. Chen, S. Ju, S. Ni, Y. Shen, Prediction methodology for ground vibration induced by passing trains on bridge structures, *Journal of Sound and Vibration* 302 (2007) 806–820.
[13] M. Dalenbring, Validation of estimated isotropic viscoelastic material properties and vibration response prediction, *Journal of Sound and Vibration* 265 (2003) 269–287.
[14] P. Avitabile, F. Piergentili, Consideration for effects of rotational degrees of freedom for hybrid modeling applications, *Proceedings of the Fifteenth International Modal Analysis* Conference, Orlando, FL, February 1997.
[15] J.E. Mottershead, A. Kyprianou, H. Ouyang, Structural modification—part 1: rotational receptances, *Journal of Sound and Vibration* 284 (1–2) (2005) 249–265.

[16] J.E. Mottershead, M.G. Tehrani, D. Stancioiu, S. James, H. Shahverdi, Structural modification of a helicopter tailcone, *Journal of Sound and Vibration* 298 (2006) 366–384.
[17] W. Duncan, The admittance method for obtaining the natural frequencies of systems, *Philosophical Magazine* 32 (1941) 401–409.
[18] R. Bishop, D. Johnson, *The Mechanics of Vibration*, Cambridge University Press, Cambridge, 1960.
[19] J. Mottershead, Y. Ram, Inverse eigenvalue problems in vibration absorption: passive modification and active control, *Mechanical Systems and Signal Processing* 20 (2006) 5–44.
[20] Y. Ram, S. Braun, An inverse problem associated with modification of incomplete dynamic systems, *Journal of Applied Mechanics* 58 (1991) 233–237.
[21] C. Yang, D. Adams, S. Yoo, H. Kim, An embedded sensitivity approach for diagnosing system-level noise and vibration problems, *Journal of Sound and Vibration* 269 (2004) 1063–1081.
[22] T. Johnson, C. Yang, D. Adams, S. Ciray, Embedded sensitivity functions for characterizing structural damage, *Journal of Smart Materials and Structures* 14 (2005) 155–169.
[23] C. Yang, D. Adams, S. Ciray, System identification of nonlinear mechanical systems using embedded sensitivity functions, *ASME Journal of Vibration and Acoustics* 127 (2005) 530–541.
[24] C. Yang, D. Adams, M. Derriso, G. Gordon, Structural damage identification in a mechanically attached metallic panel using embedded sensitivity functions, *Journal of Intelligent Material Systems and Structures* 19 (2008) 475–485.